Biochimica et Biophysica Acta, 777 (1984) 41–55
Elsevier

BBA 72226

CELL-CYCLE-SPECIFIC BIOSYNTHESIS OF THE PHOTOSYNTHETIC MEMBRANE OF *RHODOPSEUDOMONAS SPHAEROIDES*

STRUCTURAL IMPLICATIONS

GRACE S.L. YEN *, BRIAN D. CAIN ** and SAMUEL KAPLAN ***

Department of Microbiology, University of Illinois at Champaign-Urbana, Urbana, IL 61801 (U.S.A.)

(Received January 3rd, 1984)
(Revised manuscript received May 8th, 1984)

Key words: Cell cycle; Chromatophore; Photosynthetic membrane; Freeze-fracture; Electron microscopy; (R. sphaeroides)

Structural changes association with the intracytoplasmic membrane during the cell cycle of the photosynthetic bacterium *Rhodopseudomonas sphaeroides* have been studied by freeze-fracture electron microscopy. The isolated intracytoplasmic membrane vesicles, chromatophores, were fused in order to obtain large fracture faces, allowing more precise measurements and statistical analysis of both intramembrane particle density and size determinations. The intramembrane particle density of the protoplasmic face (PF) of the intracytoplasmic membrane, (from 4970 to 8290/μm^2), was shown to be a linear function of the protein/phospholipid ratio (from 2.5 to 5.1, w/w) of the intracytoplasmic membrane. Under constant light intensity, both the average particle size and particle size distribution remained unchanged during the cell cycle. These results provide the structural basis for the earlier reported cell-cycle-specific variations in both protein/phospholipid ratio and alternation in phospholipid structure of the intracytoplasmic membrane of *R. sphaeroides* during photosynthetic growth. The average particle diameter in the PF face of the intracytoplasmic membrane was 8.25, 9.08 and 9.75 nm at incident light intensities of 4000, 500 and 30 ft·cd, respectively. When chromatophores were fused with small, unilamellar liposomes, the intramembrane particle density decreased as input liposome phospholipid increased, whereas the particle size remained constant and particle distribution became random.

Introduction

The facultative photoheterotroph *Rhodopseudomonas sphaeroides*, capable of respiration under aerobic conditions and photosynthesis under anaerobic conditions in the presence of light, provides an excellent system for the study of membrane biogenesis as well as membrane structure-function relationships. Upon a shift from aerobic to anaerobic growth conditions in the presence of light, the cell develops an extensive intracytoplasmic membrane arising as invaginations from the preexisting cytoplasmic membrane; the intracytoplasmic membrane contains the complete photosynthetic apparatus. The amount of intracytoplasmic membrane as well as the relative proportions of the various components of the photosynthetic apparatus are regulated by the available

* Current address: Department of Microbiology and Immunology, University of California, Berkeley, CA 94720, U.S.A.
** Current address: Department of Biological Sciences, Stanford University, Stanford, CA 94305, U.S.A.
*** To whom all correspondence should be addressed.

Abbreviations: BChl, bacteriochlorophyll; LHC, light-harvesting complex.

light intensity [1–4]. Three pigment-protein complexes have been identified within the membrane and can be isolated in a functional state. These are the two light-harvesting complexes, designated LHC I and LHC II and the reaction center. LHC I occurs in fixed proportion to the reaction center [2] and is thought to be an essential intermediate in the transfer of exciton energy from the variable antenna complex, LHC II to the reaction center [5]. In turn, the reaction center carries out primary photochemistry [6]. Whereas the reaction center and LHC I are in fixed stoichiometry [2], the LHC II complex varies inversely as a function of light intensity [1].

Following cell breakage, the intracytoplasmic membrane is isolated as resealed, uniform spherical vesicles of 55–70 nm [7–9]. These vesicles, termed chromatophores, are isolated in greater than 96% purity, employing techniques developed and routinely used in our laboratory [7,9–11] and are chemically well-defined [7,10,11]. The chromatophores are both photochemically and enzymatically active and a series of photochemical [12,13], enzymatic [14] and immunological [15,16] experiments indicate that the chromatophores are of uniform orientation but of opposite orientation with respect to the cytoplasmic membrane [12,13,17,18].

Previous studies in this laboratory [19–24] on the biosynthesis of the intracytoplasmic membrane of *R. sphaeroides* using steady-state, photosynthetically grown, synchronously dividing cell populations revealed the following changes associated with intracytoplasmic membrane synthesis during the cell division cycle: (1) discontinuous decrease in the specific density of the intracytoplasmic membrane after a shift of the cell culture from ^2H_2O-to-H_2O-based medium, (2) continuous insertion of protein and photopigments into preexisting intracytoplasmic membrane, (3) large increase in the rate of cellular phospholipid synthesis prior to cell division, (4) sharp increase in the rate of phospholipid incorporation into the preexisting intracytoplasmic membrane, concurrent with the onset of cell division followed by the absence of phospholipid accumulation into the intracytoplasmic membrane throughout the remainder of the division cycle, (5) cyclical changes of the chromatophore protein/phospholipid ratio which correlate to the correspondingly cyclical changes of chromatophore intrinsic specific density, and to the chromatophore microviscosity as determined by the use of the fluorescent probe, α-parinaric acid and, (6) discontinuous increases in the succinate dehydrogenase and NADH – oxidase activities which are present at low levels in the chromatophores.

Similar observations have been reporeted although not as extensively documented or as throughly investigated for other biological membranes. For example, the discontinuous accumulation of cellular phospholipid was demonstrated in *Escherichia coli* [25,26], in neoplastic mast cells [27] and recently in yeast [28]. Furthermore, significant variations in the yeast mitochondrial protein/phospholipid ratio and a stepwise increase in the cellular cytochrome *c* oxidase activity in yeast have also been observed [28,29].

The current study presents an examination of the influence of naturally changing the membrane protein/phospholipid ratio on the structural organization of a highly purified biological membrane, the intracytoplasmic membrane of *R. sphaeroides*. This investigation represents an overall effort to relate within a single native membrane system an electron microscopic analysis of membrane structure during its biosynthesis with biochemical, biophysical and functional studies [19–24] of the same experimental material. In this paper, we report our efforts to relate the cell-cycle-specific change in protein/phospholipid ratio of the intracytoplasmic membrane with the density and/or size of the intramembrane particles associated with the intracytoplasmic membrane as revealed by freeze-fracture electron microscopy.

It has been demonstrated [30–32] that the intramembrane particles associated with the PF face of the photosynthetic membrane in several photosynthetic bacteria most likely represent macromolecular complexes consisting of the reaction center, LHC I and LHC II bacteriochlorophyll-protein complexes. Additional evidence in support of this concept from studies in *R. sphaeroides* is also reported in this paper. In order to detect small changes in particle density, the technique of rotary shadowing [33] instead of the conventional unidirectional shadowing was employed in the preparation of freeze-fracture replicas.

Materials and Methods

Organism and culture conditions. R. sphaeroides strain 2.4.1 was grown in Sistrom's minimal medium A [19]. Photoheterotrophic growth was conducted in either completely filled screw-capped vessels of 170 ml, in 1-l Roux bottles or in 5-l Povitsky bottles, under an atmosphere of 95% N_2 and 5% CO_2 with continuous sparging employing a MK 1 mass flow controller. Illumination was provided by a bank of Lumiline lamps (General Electric) placed on both sides of the vessel. Light energy was measured at the center of the vessel with a Yellow Spring Kettering model 65A radiometer through a Corning colored-glass filter (CS No. 7-69; 620–1100 nm). Light intensity was measured with a Lunasix light meter. Incubations were conducted in a plexiglass water bath at 32 °C ± 0.2 with temperature regulated by Haake FT. Cells previously adapted to the exponential phase of growth were the inoculum for asynchronous cultures. Inocula for synchronous cultures were adapted as described below. Culture turbidity was followed as described previously [9]. Asynchronous cultures were harvested at 100 Klett units using the No. 66 filter corresponding to approx. $1.5 \cdot 10^9$ cells/ml and stored as a cell paste at −20 °C until used.

Synchronization technique and cell enumeration. Populations of synchronously dividing cells were obtained by the stationary phase cycling technique of Cutler and Evans [34] as modified by Lueking et al. [19]. An asynchronous culture adapted to exponential growth was allowed to complete one mass doubling following cessation of exponential growth (approx. 360 Klett units). A portion of the culture was then transferred to 700 ml of fresh medium to give a final culture turbidity equivalent to one-eighth of the inoculum. Cells of this second cycle allowed to reach a culture turbidity identical to that of the previous culture were then used to inoculate a Povitsky bottle containing 4 l of the same medium. Samples were removed every 20 min to formaldehyde and counted immediately with 400–800 cells counted per determination.

Isolation and fusion of chromatophores. Highly purified chromatophores were isolated from whole cells according to the procedures routinely used in our laboratory [7,9,10]. Fusion of purified chromatophores employing poly(ethylene glycol) 6000 as fusogen were conducted as described previously [9]. The total population of fused chromatophores was then used for all subsequent determinations of protein, phospholipid, bacteriochlorophyll (BChl) and in freeze-fracture analyses.

Preparation of liposomes. Whole cell phospholipids were extracted from an asynchronous culture of *R. sphaeroides* 2.4.1 by the method of Folch et al. [35]. The extracted phospholipids were separated from photopigments as described by Donohue et al. [36]. Extracted phospholipids were stored in chloroform at −20 °C until use. Liposomes were prepared by sonicating 30 mg of extracted phospholipids in 1.0 ml of 10 mM NaH_2PO_4 buffer (pH 7.0) in a T-80-80 model sonic bath, Laboratory Supplies, Hicksville, NY, at 28.5–33.5 °C for 15 min. The liposomes were annealed further at 60 °C for 15 min [37]. Large liposomes were pelleted by centrifugation in a Beckman 50 Ti rotor at $80\,000 \times g$ for 60 min. Small (unilamellar) liposomes were recovered by carefully withdrawing the clear supernatant as described by Barenholz et al. [38].

Fusions involving liposomes. Liposome-chromatophore fusions were conducted in the same manner as chromatophore fusions [9]. Poly(ethylene glycol) 6000 was removed by continuous and discontinuous diafiltration at 4 °C using an Amicon XM1 100A membrane filter. The dilution factor was approx. $1.5 \cdot 10^6$. Each fusion mixture was layered on a discontinuous sucrose gradient (8, 16, 24, 40% sucrose in 10 mM NaH_2PO_4, w/v, pH 7.0) and centrifuged in a Beckman SW28 rotor at $100\,000 \times g$ for 14 h at 4 °C. Distinct membrane fractions of differing density distributions were collected, while the absorbance was monitored at 365 nm. Sucrose was removed from the sample by repeated dilution and centrifugation at $80\,000 \times g$ for 2 h. Liposome fusions were conducted in the same manner as chromatophore fusions at a final concentration of 10 mg phospholipid/1.85 ml fusion mixture.

Electron microscopy-freeze fracture and negative staining. Samples for freeze-fracturing were treated with 20% glycerol as described [9]. Freeze-fracture replicas were made with a Balzers BAF 301 freeze-etch unit equipped with a rotary cold stage as described previously [9]. Freeze-fracturing was

performed at $-105\,^{\circ}C$ at a vacuum of $2 \cdot 10^{-6}$ Torr or better. A shadowing angle of 30° was chosen and a quartz thin-film monitor was used to prepare replicas of uniform thickness.

Liposomes, fused liposomes and liposome-chromatophore fusion products were negatively stained with 0.5% uranyl acetate for 3 min.

All replicas and negatively stained samples were examined in a Jeol 100C electron microscope at 80 kV with a 60 μ, objective aperture. Magnifications were calibrated with a diffraction carbon grating and pictures were taken randomly over the entire field from one or more replicas for each sample.

Particle density and size measurements. For intramembrane particle density determinations, all negatives were taken at 0° tilt and at 50000 ×, then optically enlarged to 500000 ×. A 33.4 mm test circle (corresponds to object area of 3500 nm^2) was applied to the center of an enlarged fracture face. Only PF faces whose center appeared flat, as judged by the complete symmetry of shadows in the images of particles, and whose diameter were at least twice that of the test circle were employed in measurements [39]. The number of particles enclosed by the test circle was counted and particles that intersected the circle were counted alternatively in and out. At least 50 fracture faces were analyzed and 1035–1500 particles were counted for each sample.

Much larger vesicles were obtained from chromatophore-liposome fusions when compared to chromatophore-chromatophore fusions. Therefore larger test circles (e.g., corresponding to 7000 nm^2, 10500 nm^2, 14000 nm^2, etc.) were employed for particle density determinations. In those measurements, the same rules were followed as described for chromatophore-chromatophore fusions. The total area measured for each sample was equivalent to at least seventy five 3500 nm^2 test areas.

For the measurement of intramembrane particle diameter, electron micrographs were taken at 0° tilt and at 50000 ×, enlarged to 150000 × and optically enlarged further to 120000 ×. The same criteria in selection of fracture faces for density measurement were applied to particle size measurements, i.e., only PF faces whose center appeared flat and whose diameters were at least twice that of the test circle were employed. The diameter or long axis of the intramembrane particle was measured using a calibrated ruler. A total of 400–520 particles derived from several fracture faces were measured for each sample.

Diameters of negatively stained membrane vesicles were determined using a Numonics Graphics Calculator (Landsdale, PA) interfaced to a Wang Programmable Calculator. A minimum of 200 vesicles were measured for each sample.

Analytical method. Protein concentrations were determined by a modified procedure of Lowry et al. employing bovine serum albumin as standard [40].

Phospholipid extraction of membrane preparations were conducted as described by Ames [41]. Lipid phosphorous quantitations were performed according to a simplified Morrison's method [42] with the following modifications during mineralization. 0.3 ml concentrated sulfuric acid was added to the dried phospholipid sample and incubated for 3–6 h at 160 °C. 0.1 ml concentrated H_2O_2 was then added and the samples were incubated further for 12 h at 160 °C. For conversion to micrograms of phospholipid, a molecular weight of 785 was used for the latter.

BChl was assayed by the method of Cohen-Bazire et al. [1]. Concentrations were calculated using $E_{775} = 75\ mM^{-1}$, and for conversion to micrograms of BChl, a molecular weight of 914 was used.

Results

Particle density measurements during cell cycle

We could not make reliable particle density and size measurements directly on isolated chromatophores because their small size (55–70 nm) and high radius of curvature made such analyses difficult in order to determine whether or not there is a change in the density and/or size distribution of intramembrane particles within chromatophores derived from cells at various stages of the cell-division cycle. Likewise, because of the vesicular nature of the photosynthetic membrane in situ, large flat fracture planes are not readily achievable. Therefore, we made use of our ability to fuse isolated chromatophores [9] in order to derive membrane preparations useful for the kinds of analyses envisioned.

Previous studies employing the stationary phase

cycling technique to induce division synchrony in *R. sphaeroides* have routinely employed photosynthetic cultures of 700 ml [19]. The same technique was successfully applied in achieving division synchrony in large volume cultures (4.6 l) of this organism undergoing photoheterotrophic growth. Exponential increases in total cellular mass and stepwise increases in cell number were reproducibly obtained, thereby suggesting that an adequate degree of division synchrony was achieved (data not shown). Chromatophores were isolated from small quantities of cells harvested at 20-min intervals throughout the division cycle. Protein and phospholipid content of the isolated chromatophores were determined and were shown to undergo cyclical variations as previously described in numerous other experiments from this laboratory [19–24]. Therefore, large volumes of cells for preparative analysis were harvested from synchronously dividing cell populations at strategic stages of the division cycle and highly purified chromatophores were isolated from these cells as described previously. The chromatophores were subsequently used in protein and phospholipid determinations and in fusion experiments [9]. It is important to point out that the data which are provided below represent a composite of samples taken from several synchrony experiments performed under identical conditions. The necessity of employing this approach was two-fold: (1) the volume of sample needed was substantial and (2) until an experiment was terminated, it was not obvious as to precisely where in the cell cycle the sample was derived. Once a series of synchronous cell experiments were performed, then samples representing different points in the cell cycle were taken for further study.

The purpose of the fusion procedure was to obtain chromatophores derived from any point within the cell cycle which were of larger vesicle size than the unfused preparation in order to facilitate statistical analysis of intramembrane particle density and size. The orientation and integrity of fused chromatophores thus obtained have been previously demonstrated to be identical to those of control chromatophores [9]. Protein/phospholipid ratios of each chromatophore sample before and after fusion were determined in parallel and the difference between the two ratios for each sample was less than 5–10%.

Fig. 1 is a composite of freeze-fracture faces showing the intramembrane particle density of PF faces of fused chromatophores derived from synchronously dividing cells harvested at various stages in the cell cycle. Chromatophore samples with lower protein/phospholipid ratios exhibit intramembrane particles which are less densely packed on the PF face; conversely, samples with higher protein/phospholipid ratios have intramembrane particles which are more densely distributed on the PF face. Fig. 1 shows representative examples of PF faces (more than 50 per sample) analyzed for particle density determination. Fig. 2 shows a plot of the intramembrane particle density of the PF face versus chromatophore protein/phospholipid ratio. It is evident that as the chromatophore protein/phospholipid ratio increases the overall PF face particle density increases. The protein/phospholipid ratios of chromatophores isolated from synchronously dividing cell populations ranged from 2.5 to 5.1, while the corresponding particle density ranged from 49.7 ± 0.8 to $82.9 \pm 1.2/10^4$ nm^2 (i.e., 4970 $\pm$ 80 to $8290 \pm 120/\mu m^2$). Fused chromatophores from an asynchronous culture had a protein/phospholipid ratio of 3.7 and a particle density of $66.3 \pm 1.7/10^4$ nm^2 (i.e., $6630 \pm 170/\mu m^2$). Table I is a summary of the data from Fig. 2 giving the

TABLE I

PROTEIN/PHOSPHOLIPID RATIO VERSUS PARTICLE DENSITY IN CHROMATOPHORES FROM SYNCHRONOUS CELLS

a, b, c, and d represent samples derived from different experiments.

Sample number	Protein/ phospholipid	Average number of particles per 10^4 nm^2	Confidence limits (99%)
1a	2.5	49.7	47.6–51.8
2a	3.1	61.0	58.5–63.5
2b *	3.1	60.3	57.5–63.2
3c *	3.4	67.9	65.0–70.7
4a	3.8	72.4	68.9–76.0
4b *	3.8	70.8	68.5–73.1
5d *	4.2	73.4	70.7–76.1
6c *	4.1	75.4	72.9–77.9
7d *	5.1	82.9	79.6–86.2

* Samples subsequently employed in particle density histogram analyses and particle size measurements.

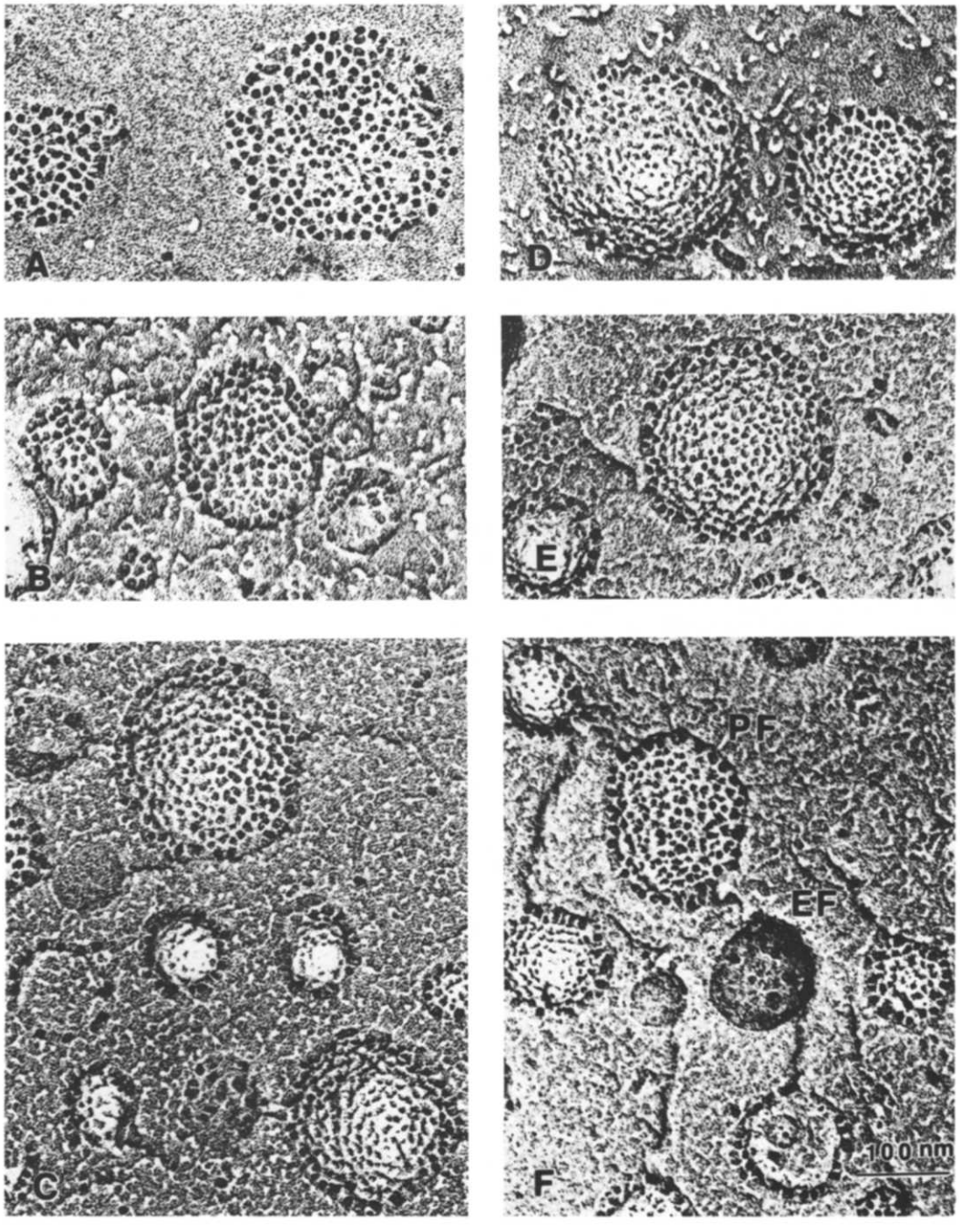

Fig. 1. Freeze-fracture replica of fused chromatophores which were derived from cell samples harvested at various stages in the division cycle from synchronous cultures of *R. sphaeroides* grown photoheterotrophically at 500 ft·cd. The protein/phospholipid ratios of chromatophore samples in A–F were 3.1, 3.4, 3.8, 4.2, 4.1 and 5.1, respectively. The fracture faces exhibit densely packed particles on PF faces and sparsely distributed particles on EF faces. Bar represents 100 nm. × 135000.

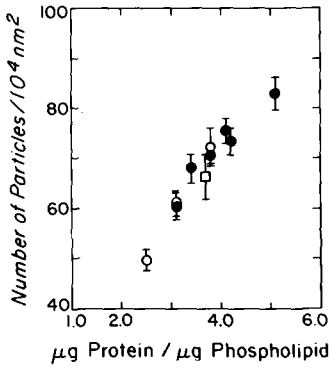

Fig. 2. Effect of chromatophore protein/phospholipid ratio on the intramembrane particle density of the PF face of fused chromatophores. Protein and phospholipid contents of purified chromatophores were determined as described in Materials and Methods. The intramembrane particle density on the PF face of purified chromatophores as revealed by freeze-fracture was measured using a 3500 nm^2 test circle as described in Materials and Methods. The raw data were then converted to number of particles/10^4 nm^2 and plotted against protein/phospholipid ratio. ○, Purified chromatophores isolated from nine culture samples in four synchrony experiments. ●, Samples subsequently employed in particle density histogram analyses and particle size measurements. □, Purified chromatophores isolated from asynchronous culture of *R. sphaeroides* grown under similar culture condition at 500 ft·cd. Bars represent 99% confidence limits.

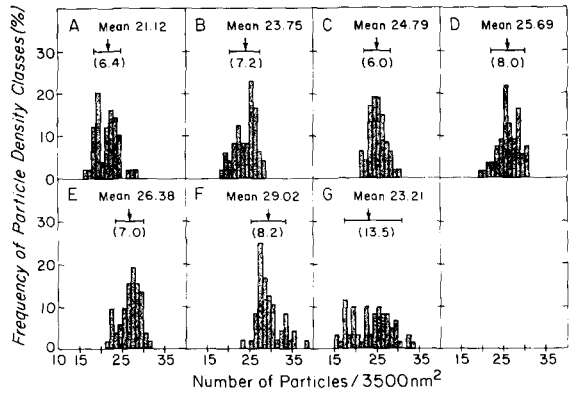

Fig. 3. PF face particle density histograms of fused chromatophores isolated from synchronous (A–F) and asynchronous (G) cultures grown photoheterotrophically. Arrow indicates the mean particle density for each sample. Horizontal bar and the number in parentheses show the distribution range of 83.3% with the median data point positioned at the mean of the sample population measured. The protein/phospholipid ratio of samples in A–G are 3.1, 3.4, 3.8, 4.2, 4.1, 5.1 and 3.7, respectively.

details of the measurements presented.

Synchronous samples represented by solid circles in Fig. 2 were subsequently employed in further particle density and size analyses. The histogram describing particle density (Fig. 3) reveals that the grouping of classes is tight and both the lower and upper density boundaries increase as the sample proceeds across the division cycle. Furthermore, 83.3% of the PF faces analyzed for each sample distributed within a density span of 6.0 to 8.2, with the median position at the mean. In contrast, no major particle density class peak was observed in the asynchronous sample, and 83.3% of the samples analyzed distributed in a density range spanning 13.5 around the mean (Fig. 3G).

Particle size measurements during cell cycle

The size distribution of intramembrane particles on the PF faces of fused chromatophores derived from both synchronous and asynchronous cultures grown under similar light conditions (500 ft − cd) were also measured. In these studies, the mean particle sizes of the samples derived from the synchronously dividing cell populations ranged from 9.02 ± 0.11 to 9.13 ± 0.12 nm and that of an asynchronous sample was 9.08 ± 0.12 nm. Particle size histograms of synchronous samples all displayed a major peak at approx. 9.0 nm with only a slight shift in the mode of the histogram (Fig. 4). Fig. 5B shows the particle size histogram of the asynchronous culture grown under similar light intensity. The histogram reveals a normal distribution with a lower but broader peak height. Furthermore, 83.3% of the total particles measured distributed within a size range of approx. 7.9 nm in the asynchronous culture versus a size range of approx. 6.2 to 6.7 nm for the synchronous samples. It is essential that we point out that the method of rotary shadowing is not as accurate as unidirectional shadowing for measuring particle diameter; see Discussion. However, it is important to note that although the distribution of particle sizes between asynchronous and synchronous samples differed, the absolute range of particle sizes, from approx. 5 to 18 nm, was identical for samples derived from both cultures.

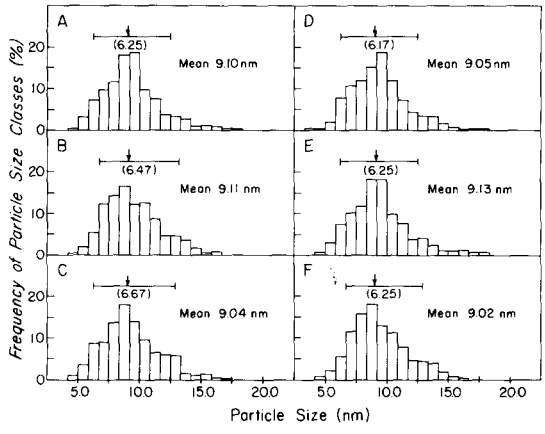

Fig. 4. Histograms of particle size classes on the PF face of chromatophores isolated from synchronous cultures grown at 500 ft·cd. Arrow indicates the mean particle size. Horizontal bar and number in parentheses show the size range in which 83.3% of the total particles measured were distributed around the mean. The protein/phospholipid ratios of samples in A–F were 3.1, 3.4, 3.8, 4.2, 4.1 and 5.1, respectively.

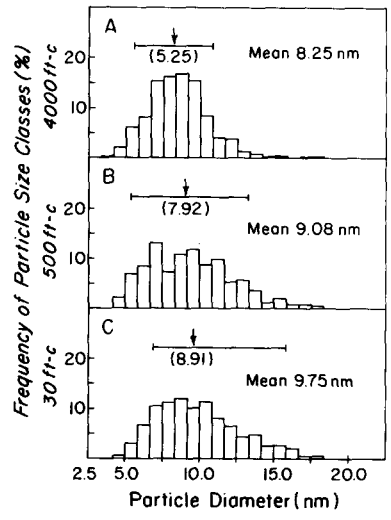

Fig. 5. Particle size histograms of intramembrane particles on the PF faces of chromatophores isolated from asynchronous cultures grown at 4000, 500 and 30 ft·cd, respectively. Arrow indicates the mean particle size. Horizontal bar and number in parentheses indicate the range of particle size distribution in which 83.3% of the particle population measured were distributed with the median data point positioned at the mean.

Effect of light intensity on structure and size distribution of intramembrane particles

We isolated chromatophores from asynchronous cultures grown at light intensities of 4000, 500 or 30 ft · cd (light energy measured was 120, 10 and 3 W/m^2), respectively and the protein/phospholipid ratio and the specific BChl content of the purified chromatophores were determined. Freeze-fracture replicas of fused chromatophores derived from the three samples were also analyzed and the results are summarized in Table II. It is evident that a decrease in the light intensity led to an increase in the generation time, an increase in the specific BChl content of the chromatophores and an increase in the mean particle size of the intramembrane particles on the PF face of the fused chromatophores, while the mean particle density remained unchanged at 4000 and 500 ft · cd and increased 10% at 30 ft · cd.

Although the appearance of a new size class peak was not observed (Fig. 5), the frequencies of

TABLE II

SUMMARY OF BIOCHEMICAL AND FREEZE-FRACTURE DATA FOR FUSED CHROMATOPHORES DERIVED FROM CELLS GROWN AT DIFFERENT LIGHT INTENSITIES

Asynchronous cultures of *R. sphaeroides* were grown at 4000, 500 or 30 ft·cd, respectively, and harvested at the same culture turbidity. The BChl, protein and phospholipid content of purified chromatophores isolated from these cultures were determined as described in Materials and Methods. Particle size and density of intramembrane particles on the PF faces of purified fused chromatophores were measured also as described.

Light intensity (ft·cd)	Generation time (h)	μg BChl/ mg protein	Average particle size (nm)	μg Protein/ μg phospholipid	Average number per 10^4 nm^2
4000	2.5	47.0	8.25 ± 0.09 [a]	2.83	68.3 ± 1.3 [a]
500	3.5	65.0	9.08 ± 0.12	3.70	66.3 ± 1.7
30	17.0	78.3	9.75 ± 0.12	3.43	74.8 ± 0.7

[a] Mean ± S.D.

smaller particle size classes decreased and those of larger particle size classes increased as the light intensity was lowered. At 4000 ft · cd, 83.3% (2σ) of the intramembrane particles measured were between 5.5 to 10.8 nm in diameter with the largest particles observed being approx. 13 nm, at 500 ft · cd the equivalent (2σ) particle size range was 5.3–13.2 nm with under 5% of the particles being greater than 14 nm and at 30 ft · cd, the corresponding (2σ) particle size range was 7.0–15.8 nm with approx. 10% of the particles being greater than 14 nm.

Chromatophore-liposome fusion

Recently, Miller [31] has elegantly demonstrated that in *Rhodopseudomonas viridis*, the photosynthetic units form a crystalline array of precisely repeating subunit structure. Although this is not so striking with *R. sphaeroides*, analysis of the particle distribution by the method of De Laat et al. [43] reveals that the particles are highly ordered and distributed within the plane of the membrane in a manner which is substantially better than random, i.e., uniform.

In order to provide a suitable control for these as well as earlier observations relating to the distribution of intramembrane particles, it was reasoned that we could artificially alter the protein/phospholipid ratio of chromatophores and, therefore, presumably the particle density and distribution by fusing chromatophores with phospholipid vesicles. Furthermore, artificially altering the protein/phospholipid ratio permitted an examination of particle density and size distributions within the PF face of the chromatophores. This was especially important, since dilution of the particles by lipid could provide information on the integrity of the particles.

Fusion of chromatophores with liposomes was performed with three different phospholipid input weight ratios, 1 : 1, 1 : 5 and 1 : 10 (chromatophore phospholipid/ liposomes phospholipid), respectively. The fusion products were resolved into distinct membrane fractions on discontinuous sucrose gradients by equilibrium density centrifugation. Major fractions from the gradients were collected and the protein and phospholipid contents of each sample were determined and are listed in Table III. The protein/phospholipid ratio of the three major peaks (A-II, B-II and C-II) decreased progressively as increasing amount of liposomes were incubated with chromatophores during fusion. The ratio also decreased progressively from fraction III to fraction I in each of the three fusions. These trends are consistent with changes in the sucrose concentration at which each of these fractions band within the gradients.

The liposomes were relatively homogeneous in vesicle size (30.0–80.0 nm) with an average diameter of 52.8 nm. Liposomes, upon fusion with one

TABLE III

SUMMARY OF PROTEIN/PHOSPHOLIPID RATIO, PARTICLE DENSITY AND SIZE, CALCULATIONS OF AREA OCCUPIED BY PARTICLES AND PARTICLE DISTANCE IN FREEZE-FRACTURE PREPARATIONS OF MEMBRANE FRACTIONS DERIVED FROM CHROMATOPHORE-LIPOSOME FUSIONS

I	II	II	IV	V	VI
Sample	μg Protein/ μg phospholipid	Average number of particles per 10^4 nm^2	Average particle size (nm)	Area occupied by particles (%)	Particle distance (Center to Center) (nm)
A-II [a]	3.18	70.7 ± 0.6 [b]	9.33 ± 0.09 [b]	48.3	13.50
B-II [a]	1.55	37.8 ± 0.7	9.33 ± 0.09	25.8	19.42
C-II [a]	1.36	40.8 ± 0.4	9.08 ± 0.10	26.4	18.56
B-I	1.14	26.3 ± 0.9	9.25 ± 0.11	17.7	24.22

[a] Major absorption peak.
[b] Mean ± S.D.

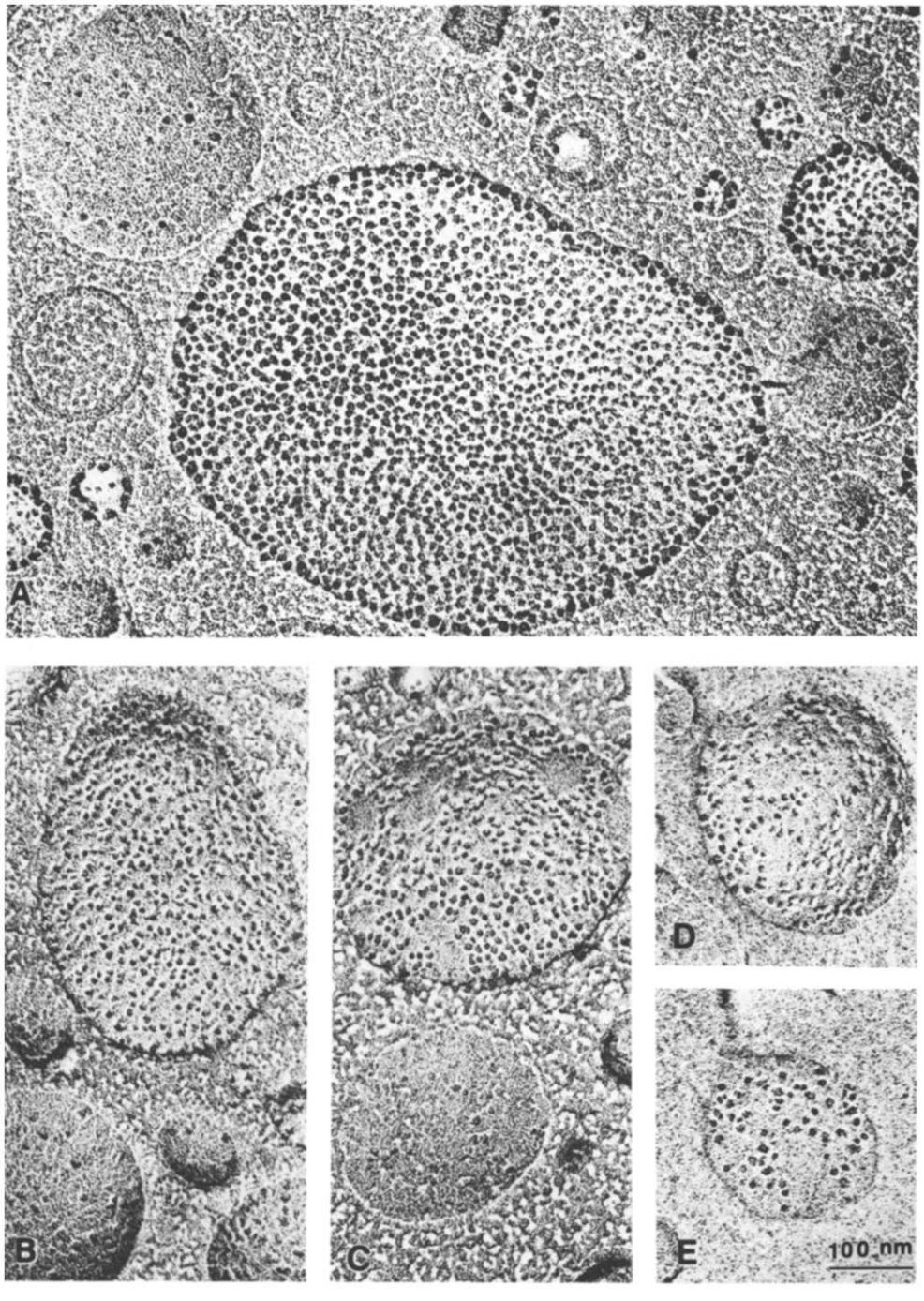

Fig. 6. High magnification electron micrographs of chromatophore-liposome fusion products. A, B and C represent Fraction A-II, B-II and C-II, respectively. Protein/phospholipid ratio was 3.18, 1.55 and 1.36, respectively. D and E represent fraction B-I (protein/phospholipid ratio was 1.14). Bar represents 100 nm. × 120000.

another, formed a heterogenous population of vesicle sizes ranging from 35.0 to 300.0 nm with a mean diameter of 101.5 nm, whereas the average diameter of purified chromatophores is 66.7 nm, as previously determined [9]. Samples obtained after liposome-chromatophore fusion consisted of vesicles of various sizes ranging from 35.0 to 300.0 nm with an average between 85.6 and 97.2 nm.

Freeze-fracture replicas were prepared from the three major pigmented peaks and B-I (Fig. 6) and the fracture faces showed a progressive decrease in particle density from the sample with high protein/phospholipid ratio to the low ratio sample. Since many more particles were observed on the concave faces than on convex faces, the former were analyzed for intramembrane particle density and size. The fracture faces of fused liposomes were smooth and did not show any intramembrane particles. The results of these studies are shown in Fig. 7 and Table III (columns II–IV). It is evident that as the fused chromatophores-liposomes were enriched with phospholipids, the particle density of the intramembrane particles decreased correspondingly, whereas particle size did not change at all.

The lateral distribution of intramembrane particles was assessed according to the quantitative method described by De Laat et al. [43] and appeared random, except for sample A-II which

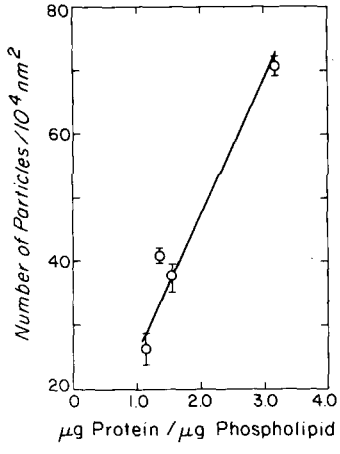

Fig. 7. Particle density on the concave fracture faces of chromatophore-liposome fusion products plotted as function of the protein/phospholipid ratio. Areas of fracture faces analyzed were equivalent to 75–148 test circle areas of 3500 nm^2. Bars represent 99% confidence limits.

was uniform. This is different from what was observed in the case of chromatophore-chromatophore fusions where the intramembrane particle distribution was significantly better than random, i.e., consistent with there being some form of substructure. Sample B-I, which had the lowest protein/phospholipid ratio among all samples analyzed, showed a slight tendency toward particle aggregation (see Discussion). The grid size (corresponding to 50 nm × 50 nm) employed in assessment of particle distribution was three-times the size of the largest particles measured [43].

Discussion

In this paper, we have analyzed the changes in the structural organization of the photosynthetic membrane of *R. sphaeroides* that occur during the cell division cycle, as well as those changes resulting from a change in incident light intensity. The technique of rotary shadowing of fractured faces enabled the visualization of intramembrane particles with greater clarity than is possible with unidirectional shadowing, although the former method is not as reliable for particle size measurement. For determination of particle density and size in the current study, small vesicles and tilted fracture faces with cast shadow were excluded. For those fracture faces large enough to be employed in particle density determination (see Materials and Methods), the test circle was applied only to the center of the fracture face, thus reducing the error in estimating surface area to less than 6% [39].

The correlation between chromatophore protein/phospholipid ratio and chromatophore intramembrane particle density strongly suggests that the insertion of new photoactive protein complexes into the intracytoplasmic membrane results in the appearance of new, distinct intramembrane particles and that there is a continuous increase in these particles within the intracytoplasmic membrane as new protein is inserted into preexisting intracytoplasmic membrane throughout the division cycle [20–22,44].

It is generally accepted that intramembrane particles revealed by freeze-fracture are protein in nature [45,46]. Our data (Fig. 2), showing the correlation between membrane protein/phospho-

lipid ratio and intramembrane particle density, coupled with the biochemical and kinetic evidence already published [19–24], strongly implies that the intramembrane particles are protein. We do not suggest that BChl is not associated with protein in the intramembrane particle, although only the contribution made by protein has been considered for the purposes of these discussions. For simplicity, we have assumed that the particles are spheres. Table IV (column VI) shows that the area covered by intramembrane particles ranged from 32.5 to 53.0% in synchronous samples with corresponding protein/phospholipid ratios changing from 2.5 to 5.1. This increase in surface area occupied by the intramembrane particles can be accounted for by a doubling in the mass of associated protein which is precisely what is observed.

Since the lateral distribution of intramembrane particles was determined to be uniform in chromatophore-chromatophore fusions, we calculated the center-to-center particle distance from 12.34 to 16.53 nm on the basis of particle density data (Table IV, column VII). Such a change might be expected to result in changes in the functional activities of vesicles with different protein/phospholipid ratios.

The observed increase in both the numerical density of particles associated with the PF face of the intracytoplasmic membrane as well as other intracytoplasmic membrane proteins not associated with the PF face as the protein/phospholipid ratio increases is consistent with the increase in membrane microviscosity [23], since it is expected that an increasing fraction of the membrane lipid would become immobilized as an increasing number of proteins (or protein complexes) are inserted into the membrane [47–51].

Particle density analysis for chromatophore-liposome fusions showed similar results to those of chromatophore-chromatophore fusions. As the protein content of chromatophore was artificially lowered by fusion with liposomes, the particle density decreased correspondingly, while the particle size remained constant. Once again, our data suggest that the intramembrane particles observed are protein in nature.

TABLE IV

SUMMARY OF PROTEIN/PHOSPHOLIPID RATIO, PARTICLE DENSITY AND SIZE, CALCULATIONS OF AREA OCCUPIED BY PARTICLES AND PARTICLE DISTANCE IN FREEZE-FRACTURE PREPARATIONS OF FUSED CHROMATOPHORES

I	II	III	IV	V	VI	VII
Sample	Light intensity (ft·cd)	μg Protein/μg Phospholipid	Average number of particles per 10^4 nm^2	Average particle size (nm)	Area covered by particles (%)	Particle distance (Center to Center) (nm)
Syn	500	2.5	49.7	9.12	32.5	16.53
Syn	500	3.1	61.0	8.94	38.3	14.68
Syn	500	3.1	60.3	9.10	39.2	14.78
Syn	500	3.4	67.9	9.11	44.3	13.81
Syn	500	3.8	70.8	9.04	45.4	13.49
Syn	500	3.8	72.4	9.00	46.1	13.32
Syn	500	4.2	73.4	9.05	47.2	13.21
Syn	500	4.1	75.4	9.13	49.4	13.02
Syn	500	5.1	82.9	9.02	53.0	12.34
Asy	4000	2.8	68.3	8.25	36.5	13.77
Asy	500	3.7	66.3	9.08	42.9	14.00
Asy	30	3.4	74.8	9.75	55.8	13.07

Syn, Synchronous sample;
Asy, Asynchronous sample.

Based on biochemical data of *R. sphaeroides* grown at 500 ft · cd it has been calculated that the chromatophore contains approximately 42 reaction center complexes, assuming the average outer chromatophore diameter as 55 nm and the inner diameter as 48 nm [4]. Our observation of 66.3 ± 1.7 particles per 10^4 nm^2 in an asynchronous sample is equivalent to 55 ± 1.4 particles per chromatophore of such size. Therefore, it is tempting to suggest that the observed intramembrane particles represent photosynthetic units consisting of reaction centers, LHC I and LHC II protein-pigment complexes. Even if the smallest of the particles observed were to represent cytochrome b-c_1 complexes, then we would have approximately 38 photosynthetic units and 19 b-c_1 complexes.

It has been shown for *R. sphaeroides* that the reaction center and LHC I are in fixed stoichiometry, while LHC II varies inversely to the incident light intensity [1,2]. In addition Takemoto and Kao [52] reported that the relative amounts of LHC polypeptides varied inversely with the light intensity. Recently Chory and Kaplan [53] demonstrated that the rates of synthesis of the LHC polypeptides associated with LHC II complexes (but not those associated with LHC I complexes) increased 4–5-fold following a 10-fold downshift in light intensity from 30 to 3 W/m^2 (500–30 ft · cd). This is commensurate with an increase in mean particle size as well as an increase in the BChl level we observed under similar culture conditions (Table II).

The procedure used for particle size determination here gives a size resolution of approx. 4 Å. The same level of resolution allows for the detection of more than one particle size class in chloroplast membranes of peas during the greening process [54]. Therefore, the lack of appearance of new particle size classes in *R. sphaeroides* as light intensity was lowered was not due to the lack of proper resolution. Both the intracytoplasmic membrane average particle size (9.0 nm) and size distribution range (5–18 nm) at 500 ft · cd were identical to those observed in a closely related photosynthetic bacterium, *R. capsulata* [55]. In those studies, the particle size determinations were performed on unidirectionally shadowed replicas. Similarly, the very narrow distribution of particle sizes from synchronous cultures clearly demonstrates the reliability of the methods we have employed. In fact, all of the data provided reinforce the reliability of these measurements. The probable reason for the validity of these measurements stems from the flatness of the fracture faces used in these studies.

The changes in particle size distribution as incident light intensity is decreased are reflected not only in an increase in the mean particle size, but also in the increased frequency of larger particles and in the relative decreased frequency of smaller particles. Furthermore, polydispersity of the particle size distribution (see Fig. 5, distribution range of 83.3% of total particles) increased as the light intensity was decreased. We suggest that the observed increase in both particle size and polydispersity are due to the increased cellular synthesis of LHC II which occurs at lower light intensities and the random association of LHC II complexes with both reaction center-LHC I complexes and reaction center-LHC I-LHC II complexes. The observation that the absolute range of particle size, from approx. 5.5 to 18.0 nm, was the same regardless of light intensity, suggests that there is an upper limit to the amount of LHC II that can be associated with any reaction center-LHC I complex. This upper limit may be dictated by the efficiency of exciton transfer from the periphery to the core of the photosynthetic unit [56–58].

Particle size analysis of fused chromatophores derived from synchronous samples showed no significant change in either the mean particle size or the size distribution in spite of the obvious changes in chromatophore protein/phospholipid ratio and particle density. Since under these conditions only the number of particles changes as a function of the protein/phospholipid ratio, we suggest that only newly synthesized reaction center and LHC I polypeptides are free to associate with one another, thereby forming new nascent core particles. On the other hand, the random incorporation and association of LHC II polypeptides implies that these are free to associate with both new and preexisting membrane particles. The net result would be a relatively constant pattern of size distributions comprised of different proportions (related to light intensity) of particle sizes despite the dynamic process of formation of new particles as well as addition of polypeptides to preexisting particles.

It is worth emphasizing that upon substantial

dilution of the photosynthetic units with phospholipid following chromatophore-liposome fusion, the size of the particles remain constant, suggesting either that once formed, LHC II subunits do not leave or exchange with other particles or that if such an exchange occurs, no free pool of LHC II units is formed.

The pattern of lateral particle distribution was determined to be uniform in chromatophore-chromatophore fusions, generally random in most chromatophore-liposome fusions where considerable dilution of the intramembrane particles, occurred, and slightly aggregative in sample B-I which had the lowest protein/phospholipid ratio among all samples analyzed. The kind of aggregative distribution suggests that the intramembrane particles have a somewhat limited degree of mobility within the chromatophore bilayer. Samples for freeze-fracture preparation were handled at room temperature for at least 1 h immediately before freezing, thus particle aggregation artifacts due to downshifts in temperature before freezing are unlikely. Furthermore, the phase transition temperature for chromatophore-phospholipid has been shown to be $-20\,^{\circ}C$ [59]. The fact that chromatophore-chromatophore fusions revealed strongly uniform particle distributions is indicative of a unique spatial arrangement of the particles relative to one another, suggesting the existence of a structural entity. Nearest neighbor analysis of particles showed that on the average, approximately six particles intersected with or were located within a circle of appropriate diameter (center-to-center particle distance) with one particle at the center of the circle, suggesting a 6-axis symmetry of particle arrangement. The very best example of such a structural arrangement has been recently demonstrated by Miller [31] for *R. viridis*.

In conclusion, we have presented detailed structural evidence which reveals that within a unique biological membrane, in situ, structural changes accompany changes in the protein/phospholipid ratio of the membrane. We have also presented evidence in support of the notion that the large intramembrane particles associated with the PF face of photosynthetic membrane are the structural counterparts of the functional photosynthetic units.

Acknowledgements

We would like to acknowledge the support from the Center for Electron Microscopy at the University of Illinois, Urbana-Champaign, in providing facilities for this study. This work was supported by Research Grant GM15590 from the USPHS.

References

1 Cohen-Bazire, G., Sistrom, W.R. and Stanier, R.Y. (1957) J. Cell. Comp. 49, 25–68
2 Aagaard, J. and Sistrom, W.R. (1972) Photochem. Photobiol. 15, 209–225
3 Kaplan, S. (1979) in The Photosynthetic Bacteria: Control and Kinetics of Photosynthetic Membrane Development (Clayton, R.K. and Sistrom, W.r., eds.), pp. 809–839, Plenum Press, New York
4 Kaplan, S. and Arntzen, C.J. (1983) in Photosynthesis, Vol. 1, Photosynthetic Membrane Structure and Function (Govindjee, ed.), pp. 65–151, Academic Press, New York
5 Thornber, J.P., Trosper, T.L. and Strouse, C.E. (1978) in The Photosynthetic Bacteria: Bacteriochlorophyll in vivo, Relationship of Spectral Forms to Specific Membrane Components (Clayton, R.K. and Sistrom, W.R., eds.), pp. 133–159, Plenum Press, New York
6 Gingras, G. (1978) in The Photosynthetic Bacteria: A Comparative Review of Photochemical Reaction Center Preparations from Photosynthetic Bacteria (Clayton, R.K. and Sistrom, W.r., eds.), pp. 119–131, Plenum Press, New York
7 Fraker, P.J. and Kaplan, S. (1971) J. Bacteriol. 108, 465–473
8 Prince, R.C., Baccarini-Melandri, A., Hauska, G.A., Melandri, B.A. and Crofts, A.R. (1975) Biochim. Biophys. Acta 387, 212–227
9 Yen, G.S.L., Wraight, C.A. and Kaplan, S. (1982) Biochim. Biophys. Acta 612, 605–621
10 Cohen, L.K. and Kaplan, S. (1981) J. Biol. Chem. 256, 5901–5908
11 Cohen, L.K. and Kaplan, S. (1981) J. Biol. Chem. 256, 5909–5915
12 Chance, B., Nishimura, M., Avron, M. and Baltscheffsky, H. (1966) Arch. Biochem. Biophys. 117, 158–166
13 Von Stedingk, L.-V. and Baltscheffsky, H. (1966) Arch. Biochem. Biophys. 117, 400–404, 537–541
14 Takemoto, J. and Bachmann, R.C. (1979) Arch. Biochem. Biophys. 185, 526–534
15 Elferink, M.G.L., Helligwerf, K.J., Michels, P.A.M., Seyen, H.G. and Konings, W.N. (1979) FEBS Lett. 107, 300–307
16 Collins, M.L.P., Mallon, D.E. and Niederman, R.A. (1980) J. Bacteriol. 143, 221–230
17 Reed, D.W. and Raveed, D. (1972) Biochim. Biophys. Acta 283, 79–91
18 Lommen, M.A.J. and Takemoto, J. (1978) J. Bacteriol. 136, 730–741
19 Lueking, D.R., Fraley, R.T. and Kaplan, S. (1978) J. Biol. Chem. 253, 451–457

20 Fraley, R.T., Lueking, D.R. and Kaplan, S. (1978) J. Biol. Chem. 253, 458–464
21 Wraight, C.A., Lueking, D.R., Fraley, R.T. and Kaplan, S. (1978) J. Biol. Chem. 253, 465–471
22 Fraley, R.T., Lueking, D.R. and Kaplan, S. (1979) J. Biol. Chem. 254, 1980–1986
23 Fraley, R.T., Yen, G.S.L., Lueking, D.R. and Kaplan, S. (1979) J. Biol. Chem. 254, 1987–1991
24 Cain, B.D., Deal, C.D., Fraley, R.T. and Kaplan, S. (1981) J. Bacteriol. 145, 1154–1166
25 Hakenbeck, R. and Messer, W. (1977) J. Bacteriol. 129, 1234–1238
26 Pierucci, D. (1979) J. Bacteriol. 138, 453–460
27 Warmsley, A.M.H., Philips, B. and Pasternak, C.A. (1970) Biochem. J. 120, 683–688
28 Cottrell, S.F., Getz, G.S. and Rabinowitz, M. (1981) J. Biol. Chem. 256, 10973–10978
29 Cottrell, S.F., Rabinowitz, M. and Getz, G.S. (1975) J. Biol. Chem. 250, 4087–4096
30 Shiozawa, J.A., Welte, W., Hodapp, N. and Drews, G. (1982) Arch. Biochem. Biophys. 213, 473–485
31 Miller, K.A. (1982) Nature 300, 53–55
32 Varga, A.R. and Staehelin, L.A. (1983) J. Bacteriol. 154, 1414–1430
33 Margaritis, L.H., Elgsaeter, A. and Branton, D. (1977) J. Cell. Biol. 72, 47–56
34 Cutler, R.G. and Evans, J.E. (1966) J. Bacteriol. 91, 469–476
35 Folch, J., Lees, M. and Sloane-Stanley, G.H. (1957) J. Biol. Chem. 226, 497–509
36 Donohue, T.J., Cain, B.D. and Kaplan, S. (1982) Biochemistry 21, 2765–2773
37 Lawaczeck, R., Kainosho, M. and Chan, S.I. (1976) Biochim. Biophys. Acta 443, 313–330
38 Barenholz, Y., Gibbes, D., Litman, B.J., Goll, J., Thompson, T.E. and Carlson, F.D. (1977) Biochemistry 16, 2806–2810
39 Weibel, E.R., Losa, G. and Bolender, R.P. (1976) J. Microsc. 107, 255–266
40 Markwell, M.A.K., Haas, S.M.,; Bieber, L.L. and Tolbert, N.E. (1978) Anal. Biochem. 87, 206–210
41 Ames, G.F. (1968) J. Bacteriol. 95, 833–843
42 Petitou, M., Tuy, F. and Rosenfeld, C. (1978) Anal. Biochem. 91, 350–353
43 De Laat, S.W., Tertoolen, L.G.J. and Bluemink, J.G. (1981) Eur. J. Cell Biol. 23, 273–279
44 Lueking, D.R., Campbell, T.B. and Burghardt, R.C. (1981) J. Bacteriol. 146, 790–797
45 Bullivant, S. (1977) J. Microsc. 111, 101–116
46 Branton, D. and Deamer, D.W. (1972) in Protoplasmatologin: Membrane structure (Alfert, M., Bauer, H., Sandritter, W. and Sitte, P., eds.), pp. 1–70, Springer-Verlag, Berlin
47 Faucon, J.-F., Dufourcq, J., Lussam, C. and Bernan, R. (1976) Biochim. Biophys. Acta 436, 283–294
48 Longmuir, K.J., Capaldi, R.A. and Dahlquist, F.W. (1977) Biochemistry 16, 5746–5755
49 Cherry, R.J., Muller, V. and Schneider, G. (1977) FEBS Lett. 80, 465–469
50 Brown, M.F., Milijanich, G.P. and Dratz, E.A. (1977) Biochemistry 16, 2640–2648
51 Curatola, W., Verma, S.P., Sakura, J.D., Small, D.M., Shipley, G.G. and Wallach, D.F.H. (1978) Biochemistry 17, 1802–1807
52 Takemoto, J. and Kao, M.Y.C.H. (1977) J. Bacteriol. 147, 354–362
53 Chory, J. and Kaplan, S. (1983) J. Bacteriol. 153, 465–474
54 Armond, P.A., Staehelin, L.A. and Arntzen, C.J. (1977) J. Cell. Biol. 73, 400–418
55 Golecki, J., Drews, G. and Buhler, R. (1979) Eur. J. Cell Biol. 18, 381–389
56 Clayton, R.K. (1967) J. Theoret. Biol. 14, 173–186
57 Van Grondelle, R., Kramer, H.J.M. and Riggersberg, C.P. (1982) Biochim. Biophys. Acta 682, 208–215
58 Pearlstein, R.M. (1983) in Photosynthesis, Vol. 1, Chlorophyll singlet excitons (Govindjee, ed.), pp. 293–330, Academic Press, New York
59 Fraley, R.T., Jameson, D.M. and Kaplan, S. (1978) Biochim. Biophys. Acta 511, 52–69